JOURNAL OF SOLID STATE CHEMISTRY 55, 150–157 (1984)

# High-Temperature Defect Structure and Electrical Conduction in $Ni_{1-x}Mg_xO$

SEUNG CHUL CHOI,* KUNIHITO KOUMOTO,
AND HIROAKI YANAGIDA

*Department of Industrial Chemistry, Faculty of Engineering, University of Tokyo, 7-3-1 Hongo, Bunkyo-ku, Tokyo 113, Japan*

Received March 13, 1984; in revised form June 11, 1984

The ionic transference number, the electrical conductivity, and Seebeck coefficient of $Ni_{1-x}Mg_xO$ ($0.1 \leq x \leq 0.9$) were measured as functions of temperature (900–1400°C) and oxygen partial pressure ($10^2$–$10^5$ Pa). The contribution of ionic conduction to the total conductivity of $Ni_{0.9}Mg_{0.1}O$ was of the order of $10^{-3}$–$10^{-2}$ at 900–1300°C, which led us to assume that the electronic conduction was predominating in $Ni_{1-x}Mg_xO$ ($x \leq 0.9$). The electrical conductivities of both undoped and Al-doped $Ni_{1-x}Mg_xO$ depended on the $\frac{1}{4}$ power of $P_{O_2}$, which indicated a significant impurity effect on the defect equilibria and was interpreted as showing that doubly ionized cation vacancies were the dominant point defects at high temperatures. Analyses of the difference in the temperature dependences of conductivity and Seebeck coefficient showed that band-like conduction took place in the NiO-rich composition range ($x \leq 0.1$), while thermally activated hopping of small polarons occurred in $Ni_{1-x}Mg_xO$ with $x \geq 0.3$. The calculated drift mobility abruptly decreased in the composition region where the conduction mechanism changed. 

## 1. Introduction

Nickel oxide is one of the 3*d* transition metal oxides which is known to be a *p*-type semiconductor at high temperatures due to its metal-deficient nonstoichiometry. For many years the investigation of electrical conduction mechanism for NiO has been performed extensively, it has resulted in giving rise to major conflicting models: thermally activated hopping of small polarons (*1–4*) and band-like conduction of holes (*5–8*). High-temperature defect structure in NiO has also been a focus of discussion due to the fact that the deviation from stoichiometry is small ($\delta$ in $Ni_{1-\delta}O$ is $\sim 10^{-3}$ at 1400°C (*9*)) and defect equilibria can easily be altered by impurities. Recent investigation by the present authors on systematically doped NiO has revealed that the conduction of electron holes takes place in a rather wide band and doubly ionized nickel vacancy is the dominant defect at 800–1400°C (*9*).

It may be expected that the electronic state in NiO should be disturbed by adding MgO in solid solution without changing the basic rock salt structure (*10*). Electronic properties of $Ni_{1-x}Mg_xO$ have been reported by several investigators. Verwey *et al.* (*11*) reported that the electronic conductivity decreased and the activation energy increased with increasing MgO content, which was also observed later by Davies

* To whom correspondence is to be addressed.

0022-4596/84 $3.00

(*12*). Austin and Gamble (*13*) found a large decrease in the drift mobility of holes with increasing $x$ in Li-doped $Ni_{1-x}Mg_xO$ at 1000 K. Choi *et al.* (*14*) measured the electronic conductivities of MgO single crystal doped with 0.375–5% NiO at different oxygen partial pressures. However, the defect structure and the conduction mechanism at high temperatures are not yet completely elucidated for $Ni_{1-x}Mg_xO$.

In the present study, the electrical conductivity and Seebeck coefficient of $Ni_{1-x}Mg_xO$ ($0.1 \leq x \leq 0.9$) were measured as functions of temperature and oxygen partial pressure to clarify the defect structure and conduction mechanism at high temperatures.

## 2. Experimental Procedure

### *2.1. Material Preparation*

Nickel oxide and MgO powders of 99.99% purity were used as starting materials. The powders were mixed in the desired proportions and pressed hydrostatically at 180 MPa. The pressed body was sintered at 1600°C for 5 hr in air. The obtained sintered compacts were cut with a diamond saw into rectangular bars, which were polished by an abrasive paper and cleaned ultrasonically with acetone and distilled water to remove surface contamination for electrical measurements. The obtained specimens had relative densities ranging from 86 to 96%.

### *2.2. Electrical Measurements*

*2.2.1 Ionic transference number.* The experimental apparatus was similar to that used by Mitoff (*15, 16*) and Sempolinski and Kingery (*17*). The ionic transference number was measured using an oxygen concentration cell arrangement. The electrodes consisted of perforated sheets of platinum superposed on the Pt–Pd sputtered films on both sides of the specimen. Oxygen partial pressure ($P_{O_2}$) on the one side of the specimen was changed from $10^2$ to $10^5$ Pa using mixtures of Ar and $O_2$, being monitored by a zirconia oxygen sensor, while $P_{O_2}$ on the other side was kept at $10^5$ Pa. The thin specimen of ca. 0.5 mm thick was used so as not to pick up thermoelectromotive force. The emf developed across the specimen was measured and the ionic transference number was calculated using the equation

$$E = \frac{RT}{4F} \int_{P_{O_2}(I)}^{P_{O_2}(II)} t_i d \ln P_{O_2}, \qquad (1)$$

where $t_i$ is the ionic transference number, $R$ the gas constant (8.314 J/K), $T$ the absolute temperature, $F$ the Faraday constant (96,900 C/eq), $P_{O_2}(I)$ and $P_{O_2}(II)$ oxygen partial pressures on the two sides of the specimen, respectively.

*2.2.2. Electrical conductivity and Seebeck coefficient.* Electrical conductivity was measured using a dc four probe technique at 900–1400°C as a function of $P_{O_2}$. The measuring system used in the present work was similar to that reported previously (*18*). Equilibrium was checked by recording the variation of a voltage drop with time during constant current supply within experimental errors. It took about 30 min for the present specimens to equilibrate depending on temperature and $P_{O_2}$.

Thermoelectric power measurements were performed at $P_{O_2} = 10^5$ Pa varying temperature. The specimen was set in the middle of the furnace and temperature gradient in the specimen was generated by the cool air flowing in an alumina protection tube placed near the one end of the specimen. The temperature difference between the two points was controlled to be 2–10 K by varying the flow rate of air, while the average temperature of the specimen was fixed. Plots of thermoelectric power vs temperature difference gave rise to a straight line in all cases, and Seebeck coefficient was calculated from its slope.

## 3. Results and Discussion

### 3.1. Ionic Transference Number

The emf's of an oxygen concentration cell for $Ni_{0.1}Mg_{0.9}O$ are shown in Fig. 1. As seen in the figure the emf is proportional to the logarithm of the oxygen potential difference at a fixed temperature, which indicates that the $t_i$ in Eq. (1) is independent of $P_{O_2}$ at least in the present $P_{O_2}$ range. Hence, the $t_i$'s could be calculated from the slopes of the straight lines in the figure. The temperature dependence of $t_i$ for $Ni_{0.1}Mg_{0.9}O$ is shown in Fig. 2. The $t_i$ increased with increasing temperature from 4 $\times 10^{-3}$ to 1.3 $\times 10^{-2}$ which is considerably small compared with that in an undoped MgO single crystal reported by Mitoff (*15*) and Sempolinski and Kingery (*17*). Calculated electronic and ionic conductivities for $Ni_{0.1}Mg_{0.9}O$ are shown in Fig. 3. The activation energy for ionic conduction is 210 kJ/mole which is comparable to that of the Mg vacancy diffusion in MgO single crystal (~220 kJ/mole (*17*)), while the activation energy for electronic conduction is 153 kJ/mole. Since it may be expected that the contribution of ionic conduction to the total conductivity decreases with increasing NiO concentration, it will be assumed for further discussion that the electronic conduction is predominating in the composition range $0.1 \leq x \leq 0.9$ in $Ni_{1-x}Mg_xO$.

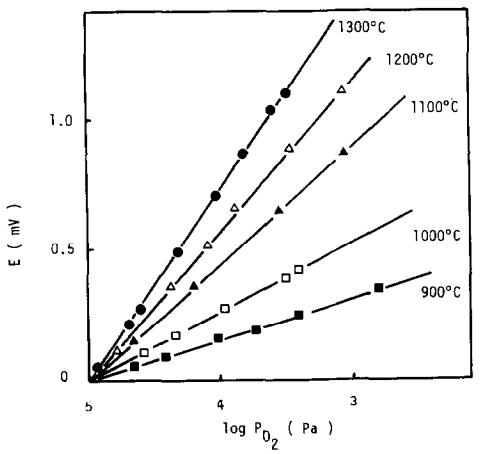


FIG. 1. Oxygen partial pressure dependence of the emf for $Ni_{0.1}Mg_{0.9}O$.

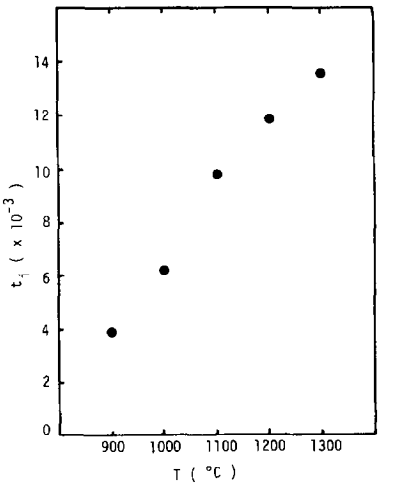


FIG. 2. Temperature dependence of the transference number for $Ni_{0.1}Mg_{0.9}O$.

### 3.2. High-Temperature Defect Structure

At temperatures high enough for the

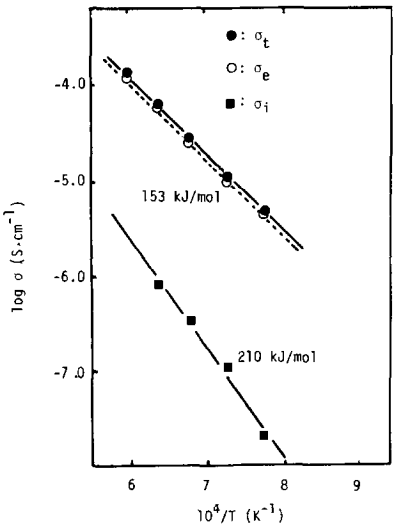


FIG. 3. Electronic and ionic conductivities for $Ni_{0.1}Mg_{0.9}O$; $\sigma_t$, $\sigma_e$, and $\sigma_i$ are total, electronic, and ionic conductivities, respectively.

specimen to equilibriate with the gas phase, cation vacancies are introduced into $Ni_{1-x}Mg_xO$ according to the quasichemical reactions

$$\tfrac{1}{2}O_2 = O_O^x + V_M^x \quad (2)$$

$$V_M^x = V_M' + h^\cdot \quad (3)$$

$$V_M' = V_M'' + h^\cdot \quad (4)$$

The defect notations here are similar to those used by Kröger and Vink (*19*). Taking $K_1$, $K_2$, and $K_3$ as equilibrium constants for the reactions (2), (3), and (4), respectively, a mass action law, assuming an ideal behavior of defects, would give rise to the relations

$$[V_M^x] = K_1 P_O^{1/2} \quad (5)$$

$$[V_M']p = K_2[V_M^x] \quad (6)$$

$$[V_M'']p = K_3[V_M'] \quad (7)$$

where [ ] denotes the concentration and $p$ is the hole concentration. The hole concentration, $p$, is approximated by the electroneutrality condition

$$p = [V_M'] + 2[V_M'']. \quad (8)$$

If the concentration of singly ionized cation vacancies, $V_M'$, is large compared with that of doubly ionized cation vacancies, $V_M''$, the neutrality condition of Eq. (8) can be approximated as

$$p = [V_M']. \quad (9)$$

Combining Eqs. (5), (6), and (9), the following relation can be obtained

$$[V_M'] = p = (K_1K_2)^{1/2}P_{O_2}^{1/4}. \quad (10)$$

Similarly, the following equation can be obtained if the doubly ionized cation vacancies, $V_M''$, are predominating,

$$[V_M''] = p/2 = (K_1K_2K_3/4)^{1/3}P_{O_2}^{1/6}. \quad (11)$$

Defect structure can be estimated from the $P_{O_2}$ dependence of a certain property reflecting the concentration of either cation vacancies or electron holes, such as diffusion coefficient of cation vacancies or electronic conductivity. In the present study the $P_{O_2}$ dependences of electronic conductivity, $\sigma$, were measured and the results are shown in Fig. 4. The $\sigma$ is approximately proportional to $P_{O_2}^{1/4}$, which suggests that singly ionized cation vacancies would be the predominating point defects in $Ni_{1-x}Mg_xO$ if the impurities were not to disturb the defect equilibria. However, the impurity effect must be taken into consideration, since the deviation from stoichiometry in $Ni_{1-x}Mg_xO$ should be small as was the case for an undoped NiO (*9*).

Qualitative SIMS (Secondary Ion Mass Spectrometry, Hitachi IMA-2AS) analysis on the specimen performed after the electrical measurements showed that Al, Si, Na, and Ca were contained as impurities. As it may be possible that the specimen has picked up Al as a main impurity in the firing

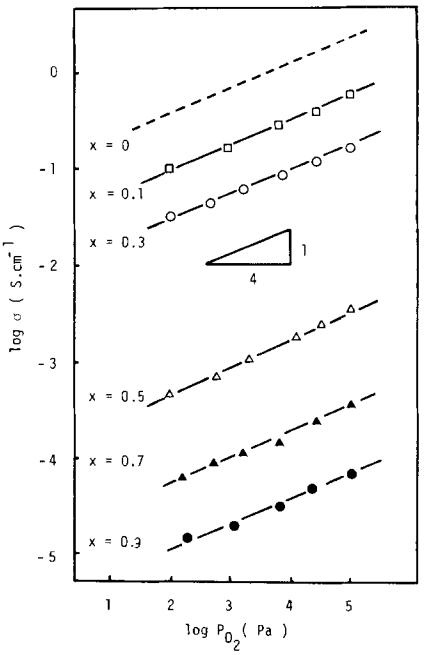


FIG. 4. Oxygen partial pressure dependences of electrical conductivity for $Ni_{1-x}Mg_xO$ at 1300°C. The dashed line is for undoped polycrystalline NiO (*9*).

process and also during the electrical measurements (*9*), the specimen of 0.15 mole% $Al_2O_3$-doped $Ni_{0.9}Mg_{0.1}O$ was prepared to further check the impurity effect. The $P_{O_2}$ dependence of $\sigma$ for Al-doped $Ni_{0.9}Mg_{0.1}O$ at 1300°C is shown in Fig. 5 with that for undoped $Ni_{0.9}Mg_{0.1}O$ for comparison. It is seen that the $P_{O_2}$ dependence of $\sigma$ was not affected by Al doping, though $\sigma$ itself decreased a little as expected. Although the solubility of $Al_2O_3$ in $Ni_{0.9}Mg_{0.1}O$ at 1300°C is not known, the present Al doping level ($3 \times 10^{-3}$ cation fraction) was explicitly assumed to be below the solubility limit; the extrapolation of the solubility of $Al_2O_3$ in NiO at high temperatures reported by Minford and Stubican (*20*) to the lower temperature region showed the solubility at 1300°C to be ~0.45 mole% ($9 \times 10^{-3}$ cation fraction), while the solubility of $Al_2O_3$ in MgO at 1300°C was calculated to be ~50 ppm ($10^{-4}$ cation fraction) (*21*). If the Al ions are substitutionally incorporated into the rock salt structure, the electroneutrality condition requires the relation

$$[V'_M] + 2[V''_M] = p + [Al_M^{\cdot}]. \quad (12)$$

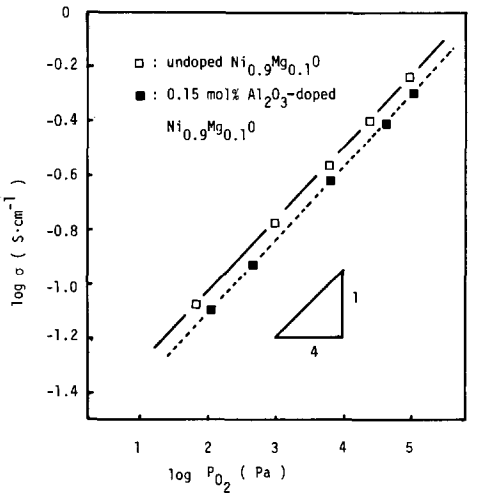


FIG. 5. Oxygen partial pressure dependences of electrical conductivity for undoped and 0.15 mole% $Al_2O_3$-doped $Ni_{0.9}Mg_{0.1}O$ at 1300°C.

The present Al doping level is considered to be much larger than the hole concentration, $p$, so that the approximation as $[Al_M^{\cdot}] \gg p$ would be reasonable (*9*). Then, if singly ionized cation vacancies, $V'_M$, are dominant, the neutrality condition is further approximated as

$$[V'_M] = [Al_M^{\cdot}] = \text{const.} \quad (13)$$

Combining Eqs. (5), (6), and (13) gives the relation

$$p = K_1K_2P_{O_2}^{1/2}/[Al_M^{\cdot}]. \quad (14)$$

If doubly ionized cation vacancies are dominant, Eq. (12) becomes

$$2[V''_M] = [Al_M^{\cdot}] = \text{const.} \quad (15)$$

and combining Eqs. (5), (6), (7), and (15) gives the relation

$$p = (2K_1K_2K_3/[Al_M^{\cdot}])^{1/2}P_{O_2}^{1/4}. \quad (16)$$

The result as shown in Fig. 5 that the $\sigma$ depends on $P_{O_2}^{1/4}$ in both undoped and Al-doped $Ni_{0.9}Mg_{0.1}O$ would confirm a significant impurity effect and leads us to the conclusion that doubly ionized cation vacancies, $V''_M$, are the dominant defects in $Ni_{1-x}Mg_xO$ at high temperatures.

### 3.3. *Electrical Conduction Mechanism*

The temperature dependences of electrical conductivity for $Ni_{1-x}Mg_xO$ obtained at $P_{O_2} = 10^5$ Pa are shown in Fig. 6. Electrical conductivity decreased with increasing MgO content, while the apparent activation energy increased with MgO content from 95.7 kJ/mole at $x = 0.1$ to 168 kJ/mole at $x = 0.9$.

The temperature dependences of Seebeck coefficient are shown in Fig. 7. The Seebeck coefficients appeared to be positive for all compositions, indicating that electron holes are the charge carriers in the solid solution as in NiO. Seebeck coefficient, $\alpha$, for a nondegenerate $p$-type semiconductor is expressed as

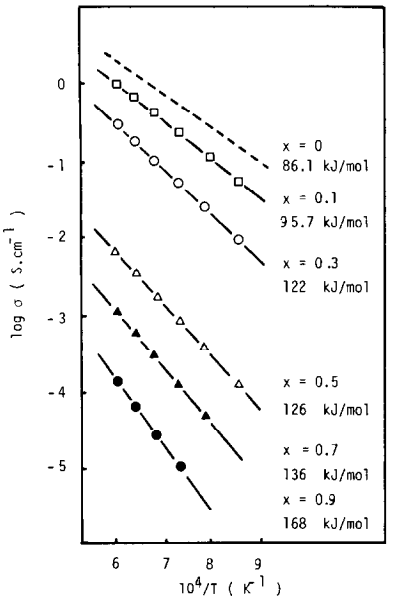


FIG. 6. Temperature dependences of electrical conductivity and its apparent activation energy for $Ni_{1-x}Mg_xO$ ($P_{O_2} = 10^5$ Pa). The dashed line is for undoped polycrystalline NiO (*9*).

$$\alpha = (k/e)\,[\ln(p_0/p) + A], \qquad (17)$$

where $p_0$ is the effective density of states at the transport level, $k$ the Boltzmann constant, and $A$ the kinetic transport term. The electronic conductivity, $\sigma$, for a $p$-type semiconductor is expressed by

$$\sigma = pe\mu, \qquad (18)$$

where $p$ is the hole concentration, $e$ the electronic charge, and $\mu$ the drift mobility of charge carriers. Differentiating Eqs. (17) and (18) with respect to $1/kT$, the following expression can be derived

$$\frac{d\log\sigma}{d(1/kT)} - \frac{d(-e\alpha/2.303\,k)}{d(1/kT)} = Q_c - Q_s = \frac{d\log\mu}{d(1/kT)} + \frac{d\log p_0}{d(1/kT)} + \frac{d(A/2.303)}{d(1/kT)} \qquad (19)$$

Equation (19) indicates that the energy difference calculated from the temperature dependences of $\sigma$ and $\alpha$ at a fixed oxygen potential gives us insight into the conduction mechanism of the material, and it has been applied to various systems, such as NiO and CoO (*22*). For a broad-band semiconductor $d\log p_0/d(1/kT) = -\frac{3}{2}kT$, which gives as the activation energy 9.6 to 13.5 kJ/mole for the temperature range 900–1400°C. For a narrow-band semiconductor $d\log p_0/d(1/kT)$ is not more than a small fraction of the hopping energy. The term $d(A/2.303)/d(1/kT)$ may be negligible in both cases (*22*). The differences in the temperature dependence of the measured conductivity and Seebeck coefficient for different compositions are shown in Fig. 8. It is seen that the apparent activation energy of conductivity, $Q_c$, increased from the value of 95.7 kJ/mole for $x = 0.1$ to a value of 168 kJ/mole for $x = 0.9$, but that of Seebeck coefficient, $Q_s$, varied a little in spite of a large composition change. As shown in Fig. 8, the energy difference, $Q_c - Q_s$, increased from 5.4 to 59 kJ/mole with an increase in $x$

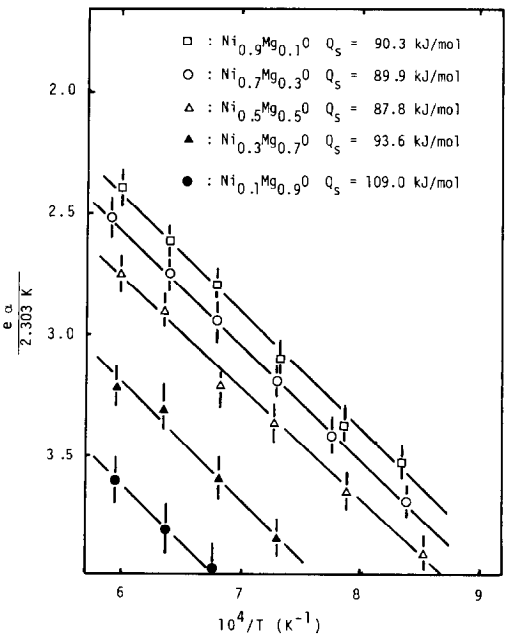


FIG. 7. Temperature dependences of Seebeck coefficient and its apparent activation energy for $Ni_{1-x}Mg_xO$ ($P_{O_2} = 10^5$ Pa).

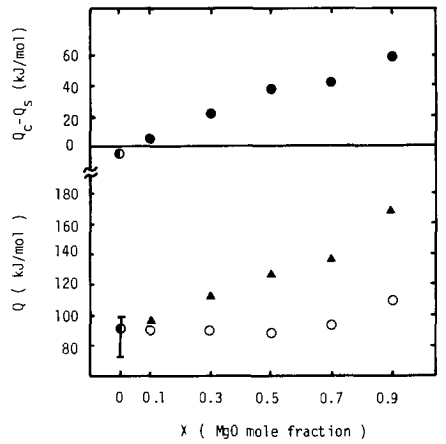


FIG. 8. Apparent activation energy for conductivity and Seebeck coefficient as a function of $x$ in $Ni_{1-x}Mg_xO$ (▲: $Q_c$, ○: $Q_s$, ◐: after Ref. (*3*), bar: $Q_c$, after various workers).

from 0.1 to 0.9. The value of $Q_c - Q_s$ for an undoped NiO also shown in the figure is approximately zero. According to the above discussion, these results may suggest that the small polarons are formed and their thermally activated hopping takes place in $Ni_{1-x}Mg_xO$ for $x \geq 0.3$, while for $x \leq 0.1$ the band-like conduction is dominant. The change in the conduction mechanism with the composition like the present case has also been reported on $Co_{1-x}Mg_xO$ (*23*), though it was later disapproved by another investigation (*24*).

The drift mobility of charge carriers can be calculated from the measured conductivity and Seebeck coefficient using Eqs. (17) and (18) on some appropriate assumptions, especially for the density of state, $p_0$, and the kinetic transport term, $A$. For a broad-band semiconductor, $p_0$ is expressed as

$$p_0 = 2(2m_h^* kT/h^2)^{3/2}$$
$$= 4.829 \times 10^{15} \times (\gamma T)^{3/2}, \quad (20)$$

where $m_h^*$ is the effective mass of an electron hole, $h$ the Planck constant, and $\gamma$ a ratio of $m_h^*$ to the mass of a free electron. For $Ni_{1-x}Mg_xO$ with $x = 0.1$ Eq. (20) was considered to be an appropriate expression to calculate $p_0$ as discussed earlier. However, the $\gamma$ value for $Ni_{1-x}Mg_xO$ is not known. Various values of $\gamma$ for undoped and Li-doped NiO have been reported ranging from 1 to 6 (*5, 8, 25, 26*), while the present authors obtained 2.4 for Al-doped NiO (*9*).

As was discussed in the previous section, the present specimen contained aliovalent impurities and the $\gamma$ value must be different from that for undoped or Li-doped NiO. Hence, $\gamma = 2.4$ obtained for Al-doped NiO was assumed to be applicable to $Ni_{0.9}Mg_{0.1}O$. For $Ni_{1-x}Mg_xO$ with $x$ larger than 0.3 where thermally activated hopping of small polarons is supposed to occur, $p_0$ was taken to be the number of $Ni^{2+}$ ions per unit volume (*22*). The kinetic transport term, $A$, was taken to be 1.6 as obtained on Li-doped NiO for band-like conduction ($x = 0.1$) and zero for hopping-like conduction ($x \geq 0.3$), as the exact value for $A$ had not been obtained. On these assumptions the drift mobility was calculated for each composition as shown in Fig. 9. Interpretation

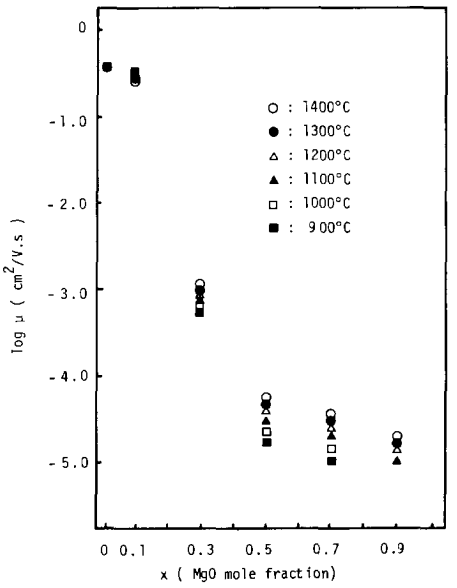


FIG. 9. Variation of the calculated drift mobility with $x$ in $Ni_{1-x}Mg_xO$. The data for $x = 0$ are from Ref. (*9*).

of a drastic change in the composition dependence of the drift mobility (conduction mechanism) should be subject to further investigation—one possible cause must be related to the fact that the distance between the two nearest $Ni^{2+}$ ions increases with increasing MgO content accompanied by a decrease in the probability for two $Ni^{2+}$ ions to exist as nearest neighbors to each other.

## 4. Conclusion

The contribution of ionic conduction to the total conductivity of $Ni_{0.9}Mg_{0.1}O$ was of the order of $10^{-3}$–$10^{-2}$ at 900–1300°C, which led us to assume that the electronic conduction was predominating in $Ni_{1-x}Mg_xO$ ($x \leq 0.9$). The electrical conductivities of both undoped and Al-doped $Ni_{1-x}Mg_xO$ depended on the $\frac{1}{4}$ power of $P_{O_2}$, which indicated a significant impurity effect on the defect equilibria and was interpreted as showing that doubly ionized cation vacancies were the dominant point defects at high temperatures. Analyses of the difference in the temperature dependences of conductivity and Seebeck coefficient showed that band-like conduction took place in the NiO-rich composition range ($x \leq 0.1$), while thermally activated hopping of small polarons occurred in $Ni_{1-x}Mg_xO$ with $x \geq 0.3$. The calculated drift mobility abruptly decreased in the composition region where the conduction mechanism changed.

## Acknowledgments

The authors are grateful to Dr. Hishita for his assistance in SIMS analysis and to Mr. Takeda for his valuable advices in experiments.

## References

1. S. P. Mitoff, *J. Chem. Phys.* **35,** 882 (1961).
2. W. C. Tripp and N. M. Tallan, *J. Amer. Ceram. Soc.* **53,** 531 (1970).
3. I. Bransky and N. M. Tallan, *J. Chem. Phys.* **49,** 1243 (1968).
4. S. Koide, *J. Phys. Soc. Jpn.* **20,** 123 (1965).
5. A. J. Bosman and C. Crevecoeur, *Phys. Rev.* **144,** 763 (1966).
6. M. B. Duff, R. Banerjee, and A. K. Barua, *Phys. Status Solidi A* **65,** 365 (1981).
7. H. J. Van Daal, *in* "Conduction in Low-Mobility Materials" (N. Klein, D. S. Tannhauser, and M. Pollak, Eds.), pp. 19–30, Taylor & Francis, Israel (1971).
8. C. M. Osburn and R. W. Vest, *J. Phys. Chem. Solids* **32,** 1331 (1971).
9. K. Koumoto, Z. Zhang, and H. Yanagida, *Yogyo Kyokai Shi* **92,** 83 (1984).
10. P. K. Davies and A. Navrotsky, *J. Solid State Chem.* **38,** 264 (1981).
11. E. J. W. Verwey, P. W. Haaijman, F. C. Romeijn, and G. W. Van Oosterhout, *Philips Res. Rep.* **5,** 173 (1950).
12. M. O. Davies, *J. Chem. Phys.* **38,** 2047 (1963).
13. I. G. Austin and R. Gamble, *in* "Conduction in Low-Mobility Materials" (N. Klein, D. S. Tannhauser, and M. Pollak, Eds.), p. 4, Taylor & Francis, Israel (1971).
14. J. S. Choi, H. Y. Lee, and K. H. Kim, *J. Chem. Phys.* **77,** 2430 (1973).
15. S. P. Mitoff, *J. Chem. Phys.* **36,** 1383 (1962).
16. S. P. Mitoff, *J. Chem. Phys.* **41,** 2561 (1964).
17. D. R. Sempolinski and W. D. Kingery, *J. Amer. Ceram. Soc.* **63,** 664 (1980).
18. K. Koumoto and H. Yanagida, *Jpn. J. Appl. Phys.* **20,** 445 (1981).
19. F. A. Kröger and H. J. Vink, *in* "Solid State Physics" (F. Seitz and D. Turnbull, Eds.), Vol. 3, p. 307, Academic Press, New York (1971).
20. W. J. Minford and V. S. Stubican, *J. Amer. Ceram. Soc.* **57,** 363 (1974).
21. W. D. Kingery, *J. Amer. Ceram. Soc.* **57,** 74 (1974).
22. I. Bransky and N. M. Tallan, *in* "Physics of Electronic Ceramics. Part A" (L. L. Hench and D. B. Dove, Eds.), p. 67, Dekker, New York (1971).
23. K. Park and E. M. Logothetis, *J. Electrochem. Soc.* **124,** 1443 (1977).
24. K. Koumoto, K. Yamayoshi, and H. Yanagida, *J. Amer. Ceram. Soc.* **66,** 42 (1983).
25. I. G. Austin, A. J. Apringthorpe, B. A. Smith, and C. E. Turner, *Proc. Phys. Soc. (London)* **90,** 157 (1967).
26. Ya. M. Kesnzov, B. K. Avedeenko, and V. V. Mararov, *Sov. Phys. Solid State* **9,** 823 (1967).